Comparative Biochemistry and Physiology, Part A 299 (2025) 111769

Contents lists available at ScienceDirect

Comparative Biochemistry and Physiology, Part A

journal homepage: www.elsevier.com/locate/cbpa

The influence of triiodothyronine on the immune response and extracellular matrix remodeling during zebrafish heart regeneration

Reece R.B. Long [a], Oliver M.N. Bullingham [a], Benjamin Baylis [b], Jared B. Shaftoe [a], John R. Dutcher [b], Todd E. Gillis [a,*]

[a] Department of Integrative Biology, University of Guelph, Guelph, Ontario, Canada
[b] Department of Physics, University of Guelph

ARTICLE INFO

Edited by: Michael Hedrick

Keywords:
Heart regeneration
Thyroid hormones
Cardiac fibroblasts
Collagen
Atomic force microscopy

ABSTRACT

Damage to the human heart is an irreparable process that results in a permanent impairment in cardiac function. There are, however, a number of vertebrate species including zebrafish (*Danio rerio*) that can regenerate their hearts following significant injury. In contrast to these regenerative species, mammals are known to have high levels of thyroid hormones, which has been proposed to play a role in this difference in regenerative capacity. However, the mechanisms through which thyroid hormones effect heart regeneration are not fully understood. Here, zebrafish were exposed to exogenous triiodothyronine (T_3) for two weeks and then their hearts were damaged through cryoinjury to investigate the effect of thyroid hormones on ECM remodeling and the components of the immune response during heart regeneration. Additionally, cardiac fibroblasts derived from trout, another species of fish known to display cardiac regenerative capacity, were exposed to T_3 *in vitro* to analyze any direct effects of T_3 on collagen deposition. It was found that cryoinjury induction results in an increase in myocardial stiffness, but this response was muted in T_3 exposed zebrafish. The measurement of relevant marker gene transcripts suggests that T_3 exposure reduces the recruitment of macrophages to the damaged zebrafish heart immediately following injury but had no effect on the regulation of collagen deposition by cultured trout fibroblasts. These results suggest that T_3 effects both the immune response and ECM remodeling in zebrafish following cardiac injury.

1. Introduction

Damage to the mammalian heart, such as what occurs during a myocardial infarction, leads to the formation of a permanent scar resulting in impaired function. In contrast, zebrafish (*Danio rerio*), axolotls (*Ambystoma mexicanum*), newts (*Notophthalmus viridescens)*, and neonatal mammals, can degrade the scar that is formed following cardiac injury and then perform complete regeneration (Becker et al., 1974; Flink, 2002; Peng et al., 2021; Porrello et al., 2011; Poss et al., 2002). Successful heart regeneration relies on the activation and crosstalk of the immune system along with the ability of cardiomyocytes to proliferate (Godwin et al., 2017). Numerous factors have been proposed to result in the unfavourable conditions for heart regeneration seen in humans including polyploidization of cardiomyocytes, reliance on aerobic metabolism in cardiomyocytes and traits of the immune system (Honkoop et al., 2019; Kimura et al., 2015; Lavine et al., 2014; Notari et al., 2018; Puente et al., 2014). Additionally, the transition to endothermy in mammals has been hypothesized to be linked to the loss of regenerative ability and is associated with greater levels of the circulating thyroid hormones triiodothyronine (T_3), and thyroxine (T_4) (Hirose et al., 2019).

Thyroid hormones act on many systems and exert different roles depending on their location of activity (Franco et al., 2011). For example, hyperthyroidism and hypothyroidism have both been found to affect the immune system (De Vito et al., 2011). More specifically, hyperthyroidism has been found to cause a reduction in the production of proinflammatory cytokines by macrophages and influences the chemotaxis of monocytes (De Vito et al., 2011). Additionally, T_3 promotes the polarization of macrophages from the M2 anti-inflammatory phenotype to the M1 pro-inflammatory phenotype and reduces the number of infiltrating macrophages in the peritoneal cavity, while increasing the number of resident macrophages in the same region (Perrotta et al.,

* Corresponding author at: Department of Integrative Biology, University of Guelph, Guelph, ON N1G 2W1, Canada.
E-mail address: tgillis@uoguelph.ca (T.E. Gillis).
@tegillis (T.E. Gillis)

https://doi.org/10.1016/j.cbpa.2024.111769
Received 16 August 2024; Received in revised form 30 September 2024; Accepted 1 October 2024
Available online 25 October 2024

2014). Thyroid hormones have also been suggested to influence the actions of various growth factors such as fibroblast growth factor (FGF) and insulin like growth factor 1 (IGF-1) (Candelotti et al., 2015). The ability of thyroid hormones to modulate components of the immune system is believed to be through the activation of cell surface integrin receptor αvβ3, which activates the MAPK pathway, rather than their classical nuclear membrane receptors (Bergh et al., 2005; Lazar, 1993). Therefore, the broad impacts of thyroid hormones appear to be related to their capacity to affect cellular processes at both the genetic and epigenetic level (Davis et al., 2018).

There have been varying reports on the role of thyroid hormones in heart regeneration. Naqvi et al. (2014) suggested that the significant increase in T_3 levels that occurs shortly after birth in mammals results in a large-scale proliferation of cardiomyocytes. To date however, these findings have not been replicated by other labs (Alkass et al., 2015; Hirai et al., 2016; Soonpaa et al., 2015). More recently, Tan et al. (2019) suggested that T_3, in conjunction with hydrogen peroxide (H_2O_2), promotes cardiomyocyte division in neonatal mice through the activation of JNK2α2, which is a mitogen-activated protein kinase (MAPK). However, T_3 has also been found to have negative impacts on heart regeneration. Hirose et al. (2019) showed that depleting the thyroid hormone receptor, TRα, in the cardiomyocytes of neonatal mice resulted in a prolonged increase in the number of diploid cardiomyocytes and improved cardiac function following damage relative to controls. This was predicted to be due to a significant reduction in the expression of carnitine palmitoyl transferase 2 (Cpt2), an enzyme involved in the breakdown of fatty acids through beta-oxidation (Ceccarelli et al., 2011; Hirose et al., 2019). This therefore suggests that T_3 inhibits the division of cardiomyocytes through binding to its nuclear receptors (Lazar, 1993). The increase in cardiomyocyte division reported by Naqvi et al. (2014) and Tan et al. (2019) may therefore be due to the downstream effects of T_3 binding to its integrin receptor and activating the MAPK pathway. At the level of the whole heart, exposing zebrafish to exogenous T_3 to mimic endogenous conditions in mammals was shown to increase cardiomyocyte polyploidization, reduce cardiomyocyte proliferation and result in an overall impairment in heart regeneration (Hirose et al., 2019). However, whether these effects were due to T_3 acting directly on cardiomyocyte proliferation or having effects beyond the cardiomyocyte has not been examined.

Circulating thyroid hormone levels increase shortly after birth in mammals as they become endothermic (Hirose et al., 2019; Naqvi et al., 2014). This correlates with the time at which heart stiffness increases and the loss of regenerative capacity occurs (Notari et al., n.d.). The purpose of this study was to determine if thyroid hormones affect heart regeneration through modifying the immune response and subsequent remodeling of the extracellular matrix (ECM). To do this, zebrafish were exposed to T_3 and then their hearts were damaged using a cryoprobe. Atomic force microscopy was then used to measure Young's modulus, as a proxy of tissue stiffness, at multiple time points following injury as myocardial stiffness has been demonstrated to increase with an increase in collagen content (Brower et al., 2006; Mujumdar et al., 2001). It was predicted that treatment with T_3 would increase tissue stiffness. These measurements were compared to those from the hearts of control fish that had undergone cardiac injury but had not been exposed to exogenous T_3. Following cardiac injury, we also examined the influence of T_3 on the expression of genes related to: cardiomyocyte proliferation, (neuregulin (*nrg1*), insulin like growth factor 1 (*igf1*)); the immune response (macrophage expressed 1 (*mpeg1*)); and ECM remodeling (matrix metalloproteinase 9 (*mmp9*); collagen type 1 alpha 1 (*col1a1*); lysyl oxidase type 1 (*loxl1*), transforming growth factor β-1 (*tgfb1*) and *vimentin*). Finally, as fibroblasts are the main cell type involved in remodeling ECM, trout (*Oncorhynchus mykiss*) cardiac fibroblasts were exposed to T_3 and the expression of gene transcripts of proteins related to the regulation of collagen (*col1a1, mmp9;* matrix metalloproteinase 2 (*mmp2);* and tissue inhibitor of metalloproteinase 2 *(timp2*)); and the protein collagen type 1 (Col1a1) were analyzed to determine if thyroid hormones influence the ECM by directly acting upon fibroblasts (Hortells et al., 2019). Trout cardiac fibroblasts were used as they were readily available. Previous work has demonstrated that trout, like zebrafish, are capable of undergoing cardiac ECM remodeling following damage (Zena et al., 2021).

2. Methods

2.1. Animal husbandry

Wildtype adult female zebrafish (age = 8 months) were obtained from an inhouse breeding program at the Hagen Aqualab, University of Guelph and maintained in general holding tanks at 26.5–27.5 °C and a photoperiod of 12 h light:12 h dark. The fish were held at a density of 25 fish per 10 l tanks and fed Gemma 300 (Skretting, Maine, USA) twice a day. Nitrate, nitrite and ammonia levels were continuously monitored in the tanks. All experimental procedures were approved by the University of Guelph Animal Care Committee (AUP#4891) under the auspices of the Canadian Council on Animal Care (CCAC).

2.2. Overview of in vivo zebrafish T_3 exposures

Two separate experiments were performed to examine the influence of T_3 exposure on heart regeneration in zebrafish following injury. In the first experiment, 48 zebrafish were exposed to 5 nM T_3 for at least 14 days prior to injury, as conducted by Hirose et al. (2019), and then sampled on days 0, 3, 7 and 14 post-injury. These timepoints correspond to the period in which the immune response, cardiomyocyte proliferation and extensive ECM remodeling are known to occur in zebrafish following cardiac injury (González-Rosa et al., 2017). The T_3 exposure conditions were identical to those used previously (Brown, 1997; Hirose et al., 2019). Cryosections were taken from these hearts to measure their stiffness using atomic force microscopy (AFM). In the second experiment, 48 zebrafish were treated as above with T_3 and then sampled on 1, 3 and 7 days post-injury (dpi) so that the expression of gene transcripts could be measured using RT-qPCR.

2.3. Zebrafish T_3 exposure and heart cryoinjury

Zebrafish were transferred from the general holding tanks to 2 l static tanks at a density of either 3 fish/l (for the AFM experiment) or 4 fish/l (for the qPCR experiment). Water temperature was maintained at 27 °C ± 1 °C and air stones were used to maintain saturating O_2 levels. After three days of acclimation, experimental fish were exposed to T_3 as previously described by Brown (1997). In brief, a 50,000 nM stock of T_3 (Sigma, T2877) dissolved in dimethylsulfoxide (DMSO) (Fisher Scientific) was added to system water so that the final concentration of DMSO in the water was 0.01 % and the concentration of T_3 was 5 nM. The tank conditions for the control group were the same but only DMSO was added to the tank. The water in all tanks was changed daily to maintain the T_3 concentration in the experimental tanks and water quality. Following two weeks of T_3 exposure, the hearts of the treated fish and control fish were damaged using a cryoinjury procedure as outlined by Chablais and Jaźwińska (2012a, 2012b). In brief, fish were anesthetized in 0.032 % tricaine methanesulfonate (MS-222; Syndel) buffered with 0.6 g/l sodium bicarbonate and then transferred into the slit of a moist sponge. The skin and pericardium directly above the ventricle were then cut using iridectomy scissors and a liquid nitrogen cooled cryoprobe with a tip diameter of 0.8 mm was held at room temperature for 10 s and then placed directly against the beating ventricle for 24 s. UV sterilized system water was dropped onto the ventricle to thaw and remove the cryoprobe. Following cryoinjury, zebrafish were placed back in their original static tanks and allowed to recover for 3, 7 or 14 days (atomic force microscopy; $N = 6$ for each timepoint) or 1, 3 or 7 days (RT-qPCR; $N = 8$ for each timepoint). These timepoints, were chosen as they correspond to the time in which scar formation is known to occur

following cryoinjury in zebrafish (Chablais and Jaźwińska, 2012b). Zebrafish recovery was monitored closely and their swimming and feeding behaviours were observed. In total, one zebrafish was removed from the experiment due to poor recovery. To minimize infection risk post-injury, all water used for water daily changes was exposed to a UV filter.

2.4. Tissue histology

To establish that the injury protocol was damaging the ventricle, hearts were embedded in paraffin wax, sectioned at 12 μm thickness as above, then mounted onto frosted slides. Sections were then stained with Picrosirius Red to differentiate between muscle tissue, collagen, and fibrin (Junqueira et al., 1979; Whittaker and Przyklenk, 2009). Briefly, sections were rehydrated in decreasing concentrations of isopropanol (3 times in 100 %, once in 70 %, 2 min each) then water (10 min). Rehydrated sections were stained with Picrosirius Red for 90 min. Sections were then differentiated twice in acid water (2 min each) and dehydrated in isopropanol (70 % for 45 s, 100 % for 2 min each). Sections were then incubated in xylene (3 times for 2 min each). Stained slides were then imaged on a Nikon Ti2 Eclipse (Nikon, Melville, NY, USA) under brightfield and polarized light to verify the presence of an injury site using untreated zebrafish at 6, 7, and 10 dpi. Brightfield images were used to identify the region of elevated collagen and inflammation which present as dark red when stained with Picrosirius Red. Under polarized light the collagen is visible as orange, and fibrin as faint green due to birefringence (Junqueira et al., 1979; Whittaker and Przyklenk, 2009).

2.5. Preparation of hearts for atomic force microscopy and qPCR

On sampling days, the fish were euthanized in 0.1 % MS-222 buffered with 0.6 g/l sodium bicarbonate and the hearts were removed. If the heart was to be used for AFM it was exposed to 0.1 M KCl to promote maximal contraction and then transferred to cryomatrix (Epredia) and allowed to freeze on dry ice cooled ethanol. The frozen hearts were then sectioned longitudinally using a Leica cryostat at a thickness of 12 μm and thaw-mounted onto frosted slides. If the hearts were to be used for RT-qPCR they were snap frozen on dry ice and stored at −80 °C until use.

2.6. Blood collection and T_3 ELISA

The circulating T_3 levels in control zebrafish and those exposed to T_3 were measured using an ELISA kit (Eagle Biosciences, Cat# T3T31-K01) following the collection of blood plasma at 14 dpi as outlined by Babaei et al. (2013). In brief, one day prior to blood collection, the bottom tips of 0.6 ml microcentrifuge tubes were removed using a razor blade. The 0.6 ml tubes were placed in 1.5 ml tubes and soaked in 700 μl of 5.4 mg/ml heparin for 30 min. The heparin solution was discarded, and the microcentrifuge tubes were incubated at 65 °C until dry and then left to sit at room temperature overnight. The following day, zebrafish were euthanized in buffered MS-222 (0.1 % MS-222, 0.6 g/l $NaHCO_3$) on ice. The caudal fin was severed using a heparinized razor blade and the fish was placed with the wound facing down into a heparinized 0.6 ml tube sitting within a 1.5 ml tube. The tubes were then placed into a centrifuge and spun at 200 *g* for 5 min at 4 °C to collect the blood at the bottom of the 1.5 ml tube. For fish that were too big to fit into the tubes, blood was collected using heparinized capillary tubes following the methods outlined by Zang et al. (2015). The blood sample was then spun in a centrifuge at 13,700 *g* for 15 min at 4 °C to separate the plasma. The plasma was collected (approximately 4 μl per fish), transferred to a new tube then stored at −80 °C. Plasma was pooled from 1 to 3 fish and then T_3 concentrations in the blood plasma were determined following the assay instructions provided by the manufacturer.

2.7. Measurement of dry body mass

Dry mass of the treatment and control fish was determined at 14 dpi. Blood samples were first taken and then the fish were placed in an oven at 50 °C. Daily mass measurements were taken until the value became stable for 24 h (approximately 4 days post initial measurement).

2.8. Atomic force microscopy

Atomic force microscopy (AFM) measurements of the ventricle cryosections from 48 zebrafish were performed in PBS buffer using the Quantitative Imaging (QI) mode on a JPK NanoWizard Ultra Speed AFM (Bruker; Appendix Fig. 1 A). QI mode is an optimized force spectroscopy mode in which each pixel in an AFM image corresponds to a single force-distance curve (Appendix Fig. 1B and C). Measurements were performed using a NanoWorld PNP-TR Pyrex-Nitride cantilever with a nominal spring constant of 0.32 N/m and a tip radius of curvature of 10 nm as quoted by the manufacturer. A piezo z-length of 4 μm and a max force setpoint of 5 nN was used for all measurements. The point of contact between the tip and the sample was determined as a deviation from zero force using a smoothing width of 1 within the JPK Data Processing Software (version 6.1.195). The Young's modulus *E* was determined by fitting a portion of each force-distance curve to the Hertz model for a quadratic pyramidal tip (Eq. 1) within the JPK Data Processing software (Supplemental Fig. 1C):

$$F = \frac{E}{1-\nu^2}\frac{tan\alpha}{\sqrt{2}}\delta^2 \quad (1)$$

where *F* is the force on the cantilever tip, δ is the indentation depth, α is the face angle of the pyramidal tip, and ν is the Poisson's ratio of the sample which was chosen to be 0.5 (Lin et al., 2006). The portion of the force-distance curve fit to the Hertz model corresponded to an indentation depth of 1 μm as shown in the shaded grey region in Appendix Fig. 1C. The value of 1 μm was chosen such that the fitted indentation region was less than 10 % of the sample thickness (~12 μm) in accordance with Bueckle's rule to avoid any influence from the underlying substrate (Persch et al., 1994).

AFM measurements were performed on 30 μm × 30 μm scan regions of the ventricle cryosections using a pixel resolution of 128 px × 128 px for a total of 16,384 Young's modulus *E* measurements per scan (Appendix Fig. 2). For each time point, tissue sections from 6 hearts were measured using 3 to 6 scans across the whole ventricle per section, resulting in 24 to 32 scans per time point. *E* values were excluded if the fit to the Hertz model had a residual root mean square (RMS) value of more than 40 pN. This resulted in an average of 13,571 accepted *E* values per scan (average of 17 % excluded due to poor fits). For each scan region, the median value of the Young's modulus distribution (Appendix Fig. 2C) was recorded to remove the influence of a small number of larger outlier values (8 %).

2.9. Cell culture of trout cardiac fibroblasts

To characterize the influence of T_3 exposure on the regulation of collagen deposition by teleost cardiac fibroblasts, we performed experiments using cardiac fibroblasts isolated from trout heart ventricles (Johnston and Gillis, 2017). Trout cardiac fibroblasts were used in place of zebrafish cardiac fibroblasts due to difficulty associated with establishing a zebrafish cardiac fibroblast cell line. Although the capacity for heart regeneration has not been rigorously researched in trout, it has been reported that they are capable of performing extensive ventricular remodeling following coronary ligation to aid in the restoration of heart function (Zena et al., 2021).

Four previously established lines of male trout cardiac fibroblast cells were thawed and grown in Leibovitz L-15 (Gibco) supplemented with 10 % fetal bovine serum (FBS), 1 % penicillin-streptomycin and 1 %

amphotericin B (referred to as whole media) at 21 °C (Johnston and Gillis, 2017). Cells were grown in T25 flasks until the cell density was large enough to be passaged and transferred into a T75 flask. Passaging was conducted once cells had reached a confluency of 80–90 %, which occurred once a week. For passaging, whole media was removed and cells were washed in PBS prior to adding a solution of 0.25 % trypsin-EDTA and PBS at a 2:1 ratio to cause cell detachment. Once cells were visibly detached from the surface of the flask, a volume of whole media equivalent to the volume of trypsin-EDTA was added and the cell solution was centrifuged for 5 min at 500*g* and 4 °C. The cell pellet was then resuspended in whole media. In order to expose cells to T_3, 300,000 cells were placed in each well of a 6 well plate containing whole media and allowed to attach to the bottom of the well overnight. Cells were counted and checked for viability using trypan blue and a TC20 Automated Cell Counter (Bio-Rad). The next day, the media was removed, and cells were placed in pure Leibovitz L-15 overnight in order to pause the cell cycle. T_3 was dissolved in 1 M NaOH and then diluted in whole media to yield final concentrations of T_3 of either 10 nM or 70 nM, all with a concentration of NaOH equal to 20 mM. The concentrations were chosen as they represent the concentrations of T_3 reported to stimulate neonatal mouse cardiomyocyte proliferation (Naqvi et al., 2014; Tan et al., 2019). Cells were then placed in either pure whole media or whole media containing 20 mM NaOH with or without 10 nM or 70 nM T_3. Media was then replaced every 2 days to refresh the concentrations of T_3. Following the 7-day incubation, cells were prepared for either RNA or protein extraction.

2.10. Western blot analysis

The cardiac fibroblasts were harvested and then prepared for western blotting as previously described (Johnston and Gillis, 2018). Western blotting, using the rabbit anti-salmon type I collagen antibody (Cat. No. CL50171AP, Cedarlane) was completed on the resultant protein samples as previously described (Johnston and Gillis, 2018).

2.11. RT-qPCR on zebrafish ventricles and trout cardiac fibroblasts

To isolate RNA from regenerating zebrafish hearts, 4–6 ventricles were isolated and homogenized using a sonicator. The Direct-zol RNA microprep kit (Zymo Research) was then used following the provided protocol (González-Rosa et al., 2018). RNA was isolated from trout cardiac fibroblasts as previously described (Johnston and Gillis, 2017). RNA concentration and purity of all samples were determined using a Nanodrop (Thermo Fisher Scientific). cDNA was made through treating 1 μg of RNA with DNAse I followed by the use of a cDNA Synthesis Kit (Life Technologies). Approximately 10 % of the samples were run through the cDNA synthesis protocol with the exclusion of MultiScribe Reverse Transcriptase (RT) to act as the negative RT controls. Standard curves were made using primers for the genes shown in Table 1 using methods outlined by Johnston and Gillis (2017). In brief, the RT-qPCR protocol was conducted with the use of a CFX96 Touch Real-Time PCR Detection System (Bio-Rad; Hercules, California, USA) using the following settings: 10 min at 95 °C, 40 cycles of 15 s at 95 °C and 1 min at 63.3 °C, ending with a melt curve from 65.0 °C to 95 °C with increments of 0.5 °C every 5 s. Samples were run in technical triplicate at a 10× dilution and mRNA abundance relative to *β-actin* was determined using Bio-Rad CFX Manager software.

2.12. Statistical analysis

All data was analyzed using GraphPad Prism (GraphPad). An unpaired *t*-test was used to compare means between groups for the body mass and ELISA data. Median Young's modulus values were recorded from each scan and the mean value of these medians was plotted and analyzed. Two-way ANOVAs followed by a Tukey post-hoc test were conducted to compare means between groups for the AFM and *in vivo* RT-qPCR data. A one-way ANOVA followed by a Tukey post-hoc test was used to compare means between groups for the *in vitro* RT-qPCR data. Data points that were greater than two standard deviations away from the mean were removed as outliers.

Table 1
List of primers used for RT-qPCR.

Gene	Sequence (5′-3′)	Species	Efficiency (%)	R^2	Source
tgfb1	F: GCTGGTCTGGCAGATATGAT R: AGCTTGCGCATACAGCAGGT	Zebrafish	98.1	0.996	(Page et al., 2013)
igf1	F: CAGCAAACCGACAGGATATGG R: CAGCTCTGAAAGCAGCATTCG	Zebrafish	104.9	0.995	(Nelson and Van Der Kraak, 2010)
nrg1	F: CACAAATGAGTTCACATCACCA R: TCTGCTTTGCCATTACTCCA	Zebrafish	97.3	0.994	(Gemberling et al., 2015)
loxl1	F: ATCGTAGGTCACAGGGTGGA R: GAGAGCCGGTTTGTGACTGA	Zebrafish	95.8	0.992	(Che et al., 2022)
vimentin	F: ACCGGGGAAAAGAGCAAAGT R: CGAGCCAGAGAGGCGTTATC	Zebrafish	103	0.992	(LeBert et al., 2018)
mpeg1	F: CCCACCAAGTGAAAGAGG R: GTGTTTGATTGTTTTCAATGG	Zebrafish	98.9	0.997	(Ferrero et al., 2020)
mmp9	F: TACGGTAATGCTGAGGGTGC R: ATAGTCTGCGGTGGTTGAGC	Zebrafish	104.8	0.998	(Tran and Kim, 2020)
col1a1	F: TGTCACTGAGGATGGTTGCAC R: GCAGACGGGATGTTTTCGTTG	Zebrafish	97.3	0.998	(LeBert et al., 2018)
ef1a	F: GATCACTGGTACTTCTCAGGCTG R: GGTGAAAGCCAGGAGGGC	Zebrafish	99.3	0.998	(Nelson and Van Der Kraak, 2010)
β-actin	F: ACACCCGACTACCACTTCAG R: GACTGAGAAGCTGGGTTTGG	Trout	84.7	0.999	(Johnston and Gillis, 2017)
timp2	F: ACATTTTCCCTCCACGCGAT R: TTCTGCGATGTCTTCCACCC	Trout	89.9	0.997	(Johnston and Gillis, 2017)
col1a1	F: CCCGAGCCATGCCAGAT R: CGGATGTGTCCTCGCAGATAA	Trout	89.4	0.996	(Johnston and Gillis, 2017)
mmp2	F: AGACGCATAGACGCTGGCTAA R: GCAGGATAGGCTGGTTGGATAG	Trout	91.4	0.995	(Johnston and Gillis, 2017)
mmp9	F: ACCCCTTCGATGGTAAGGAC R: GGTCCAGTTTTCGTCATCGT	Trout	91.5	0.988	(Johnston and Gillis, 2017)

3. Results

3.1. Influence of T_3 exposure on plasma T_3 levels and body mass of zebrafish

The measured T_3 concentrations in the control and treated fish were 16.3 ± 12.4 nM and 52.9 ± 26.8 nM, respectively ($p > 0.05$). The T_3 exposure protocol used in the current study mimicked that of Hirose et al. (2019) where the published values, ~15 nM and ~ 25 nM, were similar to those of the current study but less variable. The source of the variability in the current study is not known. There was no difference in body mass between T_3 treated zebrafish and the control zebrafish (0.164 ± 0.008 g *vs* 0.163 ± 0.012 g).

3.2. Histology of wound site

The magnitude of an injury site varies depending on where the section is taken from (Chablais et al., 2011). Therefore, the extent of injury observed on each section can be variable; however, the histological investigation revealed that the cryoinjury procedure caused significant damage to the ventricle (Fig. 1). At 1 dpi, necrotic tissue was apparent in a large portion of the ventricle (Fig. 1B). The wound site at 1 dpi was characterized by a long, thin fibrin clot, reduced trabecular organization, which stands in stark contrast to the well-ordered and robust trabeculae around the wound site (Fig. 1B). At 7 dpi, the region of necrotic tissue was greatly reduced and replaced with a high density of collagen surrounding the fibrin clot. The periphery of the wound site

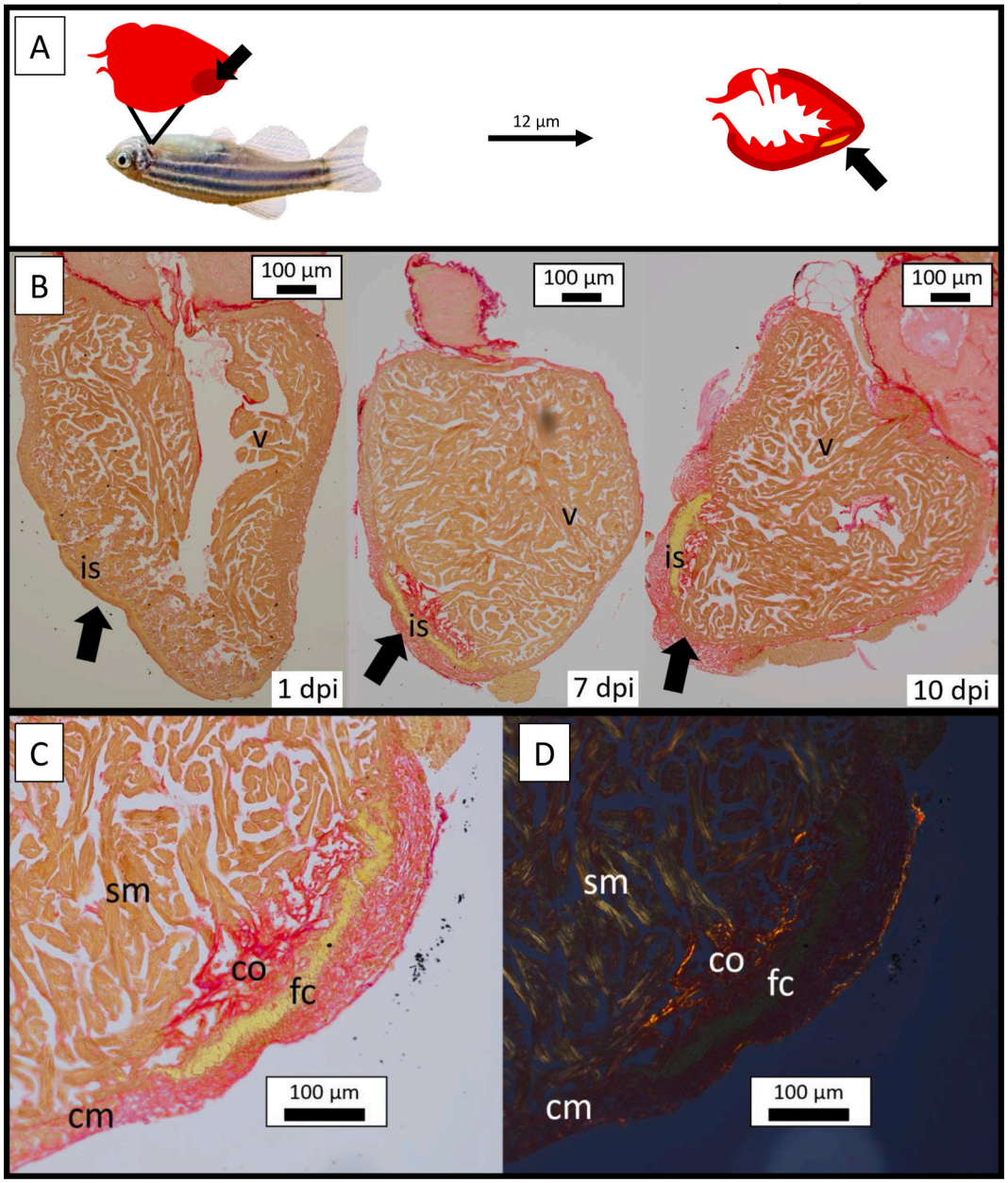

Fig. 1. Representative images of zebrafish heart post cryoinjury. (A) A super cooled probe was used to cause a cryoinjury to the ventricle in anesthetized zebrafish. The heart was then sampled at specific days post injury (dpi), sectioned along the longitudinal axis and stained with Picrosirius Red to identify the injury site. (B) Brightfield images of ventricular sections at 1-, 7-, and 10-dpi showing the injury site (is) near the apex of the ventricle (v). (C) The brightfield image at 7-dpi shows the yellow fibrin clot (fc) surrounded by brightly stained red collagen (co). (D) The polarized image highlights the densely packed (orange) collagen in the regions surrounding the faint green fibrin in the 7-dpi section. Healthy tissue of the spongy myocardium (sm) and the compact myocardium (cm) can be seen to the left of the injury site. (For interpretation of the references to colour in this figure legend, the reader is referred to the web version of this article.)

was inflamed and was darkly stained by Picrosirius Red under bright-field (Fig. 1C). The presence of collagen and fibrin were confirmed under polarized light which showed dense collagen fibres as red to orange and fibrin as faint green (Fig. 1D). At 10 dpi, the wound was similar to that at 7 dpi, presenting a fibrin clot surrounded by dense collagen and peripheral inflammation.

3.3. Influence of cardiac injury and T_3 exposure on the stiffness of the zebrafish ventricle cryosections measured using atomic force microscopy

Median Young's modulus values were recorded for the ventricle cryosections from the T_3 exposed and control zebrafish. Each data set contained four time points: undamaged (day 0), 3 dpi, 7 dpi, and 14 dpi. The measured median Young's modulus values of the ventricle cryosections of undamaged control fish are similar to those obtained from zebrafish ventricle cryosections using similar methods (Grivas et al., 2020). This indicates that the protocol used in the current study enabled successful detection of stiffness within the zebrafish ventricle. Median Young's modulus values were found to be nearly identical between the control and T_3 exposed groups prior to injury (278 ± 16 Pa and 267 ± 13 Pa respectively) (Fig. 2). Following injury, there was a significant increase in median Young's modulus values in both groups, which remained significantly elevated throughout the first 14 dpi ($P_{interaction}$ = 0.0036) (Fig. 2). At 3 dpi, median Young's modulus values were significantly greater in the control group (450 ± 27 Pa) relative to the T_3 exposed group (347 ± 17 Pa; $p < 0.05$). Finally, the median Young's modulus values were significantly higher in the control fish at 3 dpi than at 7 dpi and 14 dpi ($p < 0.05$).

3.4. Influence of cardiac injury and T_3 exposure on the expression of select gene transcripts in the zebrafish heart

There was no significant interaction between treatment and time on the expression of the gene transcript for vimentin (*vimentin*) (Fig. 3A). There was, however, a significant effect of treatment on the expression of *vimentin* with relative levels being higher in the hearts of control fish at each time point then in the hearts of the treated fish at each time point (Fig. 3A). In addition, the expression of *vimentin* was higher in the control and treated samples at 3 dpi than at 1 and 7 dpi (Fig. 3A). There was no interaction between treatment and time on the expression of *col1a1,* but there was an effect of time with the levels of *col1a1* being higher in samples from both treatment and control at 3 and 7 dpi than at 1 dpi ($p = 0.006$) (Fig. 3B). There was no interaction between treatment and time on the expression of *tgfb* but there was an effect of time with the levels of this transcript being lower in both treatment and control at 7 dpi than at 3 dpi ($p = 0.01$) (Fig. 3C). There was a significant interaction between treatment and time on the expression of *nrg1* ($P_{interaction}$ = 0.004) and there was an effect of treatment ($p < 0.003$) with the expression of the transcript in the hearts of the control fish ~2.9-fold that in the hearts of the treated fish at 1 dpi (Fig. 3D). There was no interaction between treatment and time on the expression of *loxl1* but there was an effect of time, with the expression of the transcript being lower at 7 dpi in both treatment and control than at 1 dpi ($p = 0.0037$) (Fig. 3E). There was no interaction between treatment and time on the expression of *mpeg1* but there were effects of treatment ($p < 0.003$) and time ($p < 0.008$) with the level of the transcripts being lower in the hearts of the treated fish at all time points than in the hearts of the control fish (Fig. 3F). In addition, the levels of *mpeg1* where higher in the control and treated samples at 1 dpi than at 3 and 7 dpi ($p = 0.003$) (Fig. 3F). There was no interaction between treatment and time on the expression of *mmp9* or *igf1* (Fig. 3G and H). There was however an effect of time with the levels of *mmp9* being lower in control and treatment at 7 dpi than at 1 dpi ($p = 0.048$) (Fig. 3G) and the levels of *igf1* being higher in the treatment and control at 7 dpi than at 1 dpi ($p = 0.033$) (Fig. 3H).

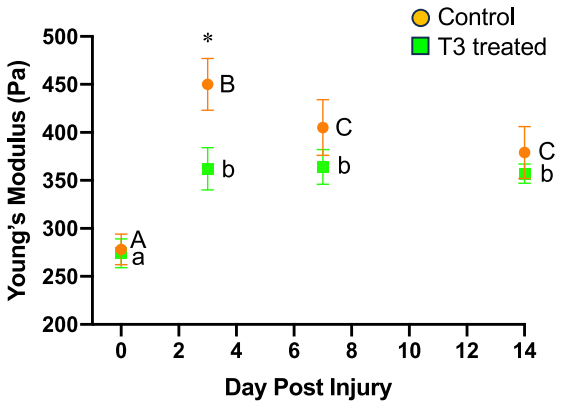

Fig. 2. The influence of T_3 exposure on the median Young's modulus values of zebrafish myocardium following injuring. $N = 6$ samples, with 3–6 scans per section. Values are presented as mean ± S.E.M. Statistical differences between mean values for the control group are indicated using capital letters and those for the treatment group are indicted with lowercase letters. Two mean values within the same group that do not share the same letter are statistically different. Asterisks indicate a difference between treatment and control at the same time point. Statistical significance was determined through a two-way ANOVA followed by a Tukey *post-hoc* test ($p < 0.05$).

3.5. Influence of T_3 exposure on the expression of select gene transcripts and Col1a1 protein in cultured trout cardiac fibroblasts

No changes in the expression of *col1a1, mmp9, mmp2 or timp2,* were observed in trout cardiac fibroblasts exposed to either 0, 10 or 70 nM of T_3 (Fig. 4a-d). There was also no effect of any T_3 concentration on the abundance of Col1a1 protein (Fig. 4e)

4. Discussion

Heart regeneration involves multiple cell types, depends on the ability of cardiomyocytes to proliferate and requires the activation of the innate immune response and collagen deposition by fibroblasts (Ryan et al., 2020). The results of the current study provide evidence that thyroid hormone is involved in regulating this integrative response, affecting the recruitment of macrophages and, as a result, the regulation of collagen deposition and stiffness of the tissue.

4.1. T_3 exposure blunted the changes in cardiac stiffness immediately following damage

The lack of difference in tissue stiffness between the ventricle cryosections from T_3 exposed fish and control fish at day 0 prior to injury suggests that 14 days of T_3 exposure did not affect biomechanical properties of the tissue. As changes in tissue stiffness can reflect collagen content (Brower et al., 2006; Mujumdar et al., 2001); this suggests that there is no difference in collagen content between the hearts from the control and the T_3 treated fish prior to injury. However, the increase in the stiffness of the ventricle cryosections from both the treatment and control groups following injury, indicates that the biomechanical properties of the tissue are affected. As an increase in ventricle stiffness reflects an increase in collagen concentration or cross-linking, this suggests that there was an increase in collagen content in the hearts of both T_3 treated and control fish. The significantly higher stiffness of the ventricle cryosections from the control fish at 3 dpi suggests that they contain more collagen than those from the T_3 treated fish. This result contrasts that of a previous study on zebrafish that showed a decrease in cardiac ECM stiffness at 7 dpi (Garcia-Puig et al., 2019). This opposite response is likely due to differences in how cardiac damage was induced. In the study by Garcia-Puig et al. (2019), the hearts were damaged using ventricular amputation whereas cryoinjury was used in the current study. With cryoinjury, the damaged tissue remains, resulting in the

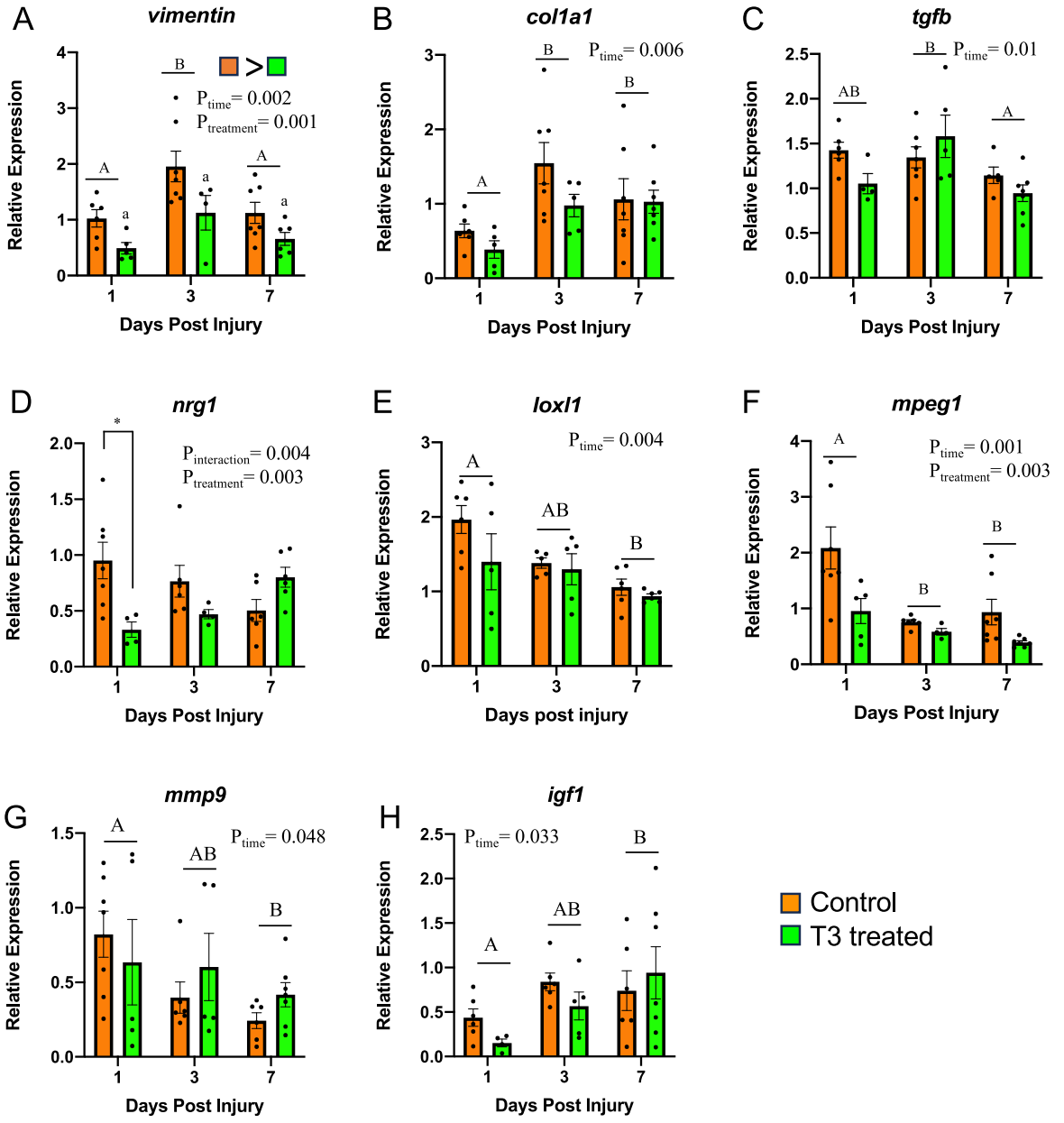

Fig. 3. The influence of T_3 exposure on the expression of various genes in the zebrafish ventricle following cryoinjury. Gene expression is normalized to *ef1a*. Orange bars represent the control group and green bars represent the T_3 exposed group. Values are presented as mean ± SEM. Pairs of bars indicated with dissimilar letters on the same panel are different from each other through time ($p < 0.05$). Overall differences in the expression of *vimentin* and *mpeg1* between treatment and control groups at all sampling points are indicated in the top right corner of the relevant panel ($p < 0.05$). An asterisk represents a difference between treatment and control at a specific time point ($p < 0.05$). Significance was determined through a two-way ANOVA followed by a Tukey *post-hoc* test ($p < 0.05$). $N = 4–7$ individual ventricles. (For interpretation of the references to colour in this figure legend, the reader is referred to the web version of this article.)

infiltration of immune cells and formation of fibrotic tissue, while with amputation a fibrin clot forms and no scarring occurs (González-Rosa et al., 2017). It has been suggested that compared to ventricular amputation, cryoinjury results in damage more akin to a myocardial infarction (González-Rosa et al., 2011). The greater stiffness measured in ventricle cryosections from the control fish compared to those from the treatment fish at day 3, suggests that T_3 exposure may blunt the fibrotic response of the heart to injury. This result was not expected as work by Hirose et al. (2019) demonstrated that the scar caused by cardiac injury measured at 28 dpi was larger in T_3 treated zebrafish then in control fish. However, the difference between the sampling times (28 dpi *vs* 3 dpi) makes the comparison of these results difficult.

4.2. Macrophage recruitment and cardiomyocyte proliferation following injury may be reduced with T_3 exposure

The gene transcript for *mpeg1* is used as a marker of macrophages (Simões et al., 2020) so the lower levels of this transcript in the T_3 exposed group at all sampling days relative to the untreated controls suggests a decrease in macrophage recruitment to the wound site following damage. In medaka, delayed recruitment of macrophages is known to impair heart regeneration through a reduction in neutrophil clearance, neovascularization and cardiomyocyte proliferation (Lai et al., 2017). Therefore, an impairment in macrophage recruitment may explain the reduced cardiomyocyte proliferation and impaired heart regeneration that was observed in T_3 exposed zebrafish by Hirose et al.

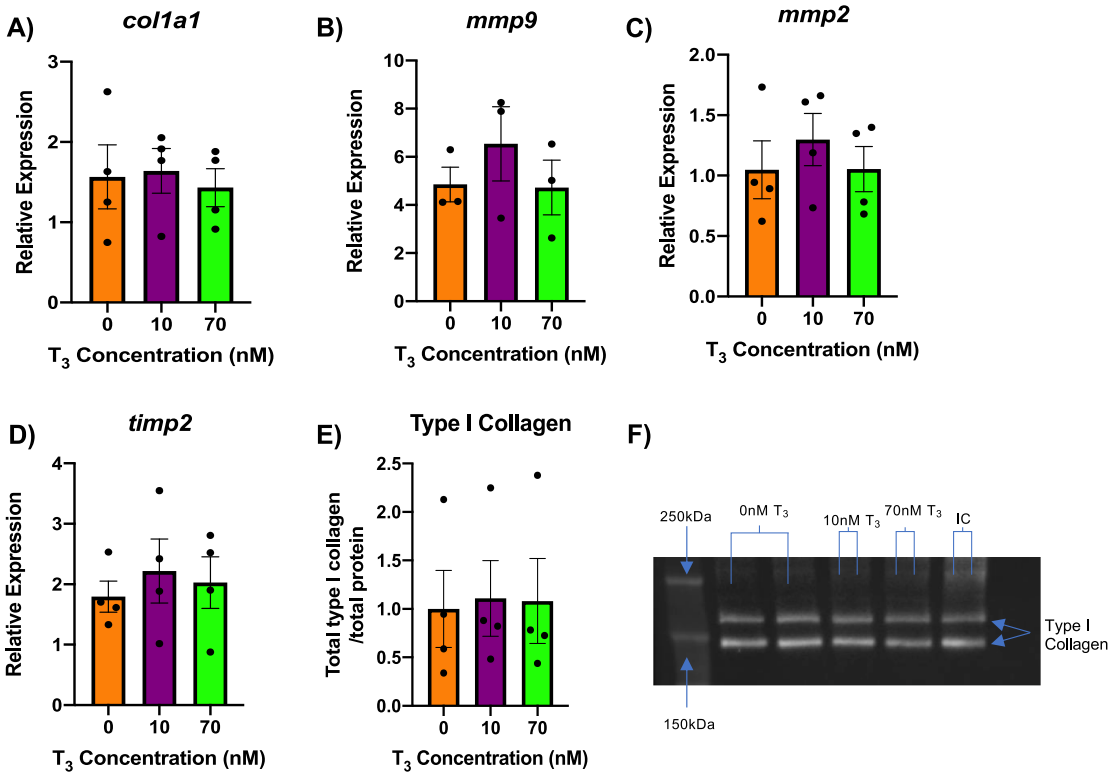

Fig. 4. The influence of T_3 exposure on the expression of select genes and type I collagen in cultured trout cardiac fibroblasts. Panels A-D) Relative expression of *col1a1, mmp2, timp2* and *mmp9*, respectively, normalized to *β-actin.* E) The expression levels of type I collagen normalized to total protein in cardiac fibroblasts. Fibroblasts were exposed to 0 nM, 10 nM or 70 nM T_3. F) Representative image of western blot stained for type I collagen. $N = 3–4$ cell lines, each individual cell line is composed of the mean of 4 cell passages. IC = internal control.

(2019). Depletion of macrophages has also been shown to impair heart regeneration in axolotls, despite having no effect on cardiomyocyte proliferation (Godwin et al., 2017). Furthermore, the recent success attributed to cardiac stem cell therapy following damage has been found to be linked to the increased activity of macrophages rather than cardiomyocyte production (Vagnozzi et al., 2020). Macrophages are also known to contribute to collagen production in zebrafish and mouse hearts following injury. Thus the reduced cardiac stiffness observed at 3 dpi in T_3 exposed zebrafish may be due to a reduction in the number of macrophages and an associated decrease in collagen production (Simões et al., 2020). This reduced stiffness may contribute to the previously observed impairment in heart regeneration as limiting the fibrotic response has been shown to impair cardiomyocyte proliferation in zebrafish (Hirose et al., 2019; Sánchez-Iranzo et al., 2018). Therefore, it is possible that T_3 may impair the regeneration process by delaying or muting the initial deposition of collagen at the wound site, which potentially could reduce the ability to remove collagen later on in the regeneration process.

Nrg1 is an injury-induced cardiomyocyte mitogen and therefore the transcript for this protein is a common marker for cardiomyocyte proliferation (Gemberling et al., 2015). The lower levels of this transcript in the hearts of T_3 exposed zebrafish at 1 dpi therefore suggests an inhibition of cardiomyocyte proliferation at that time point. This result is supported by previous work where inhibition of the actions of thyroid hormones on their respective nuclear receptors in mouse cardiomyocytes helped to maintain cardiomyocyte division, and exposing zebrafish to T_3 impairs cardiomyocyte proliferation and overall heart regeneration (Hirose et al., 2019). Igf1 is also known to play an important role in upregulating cardiomyocyte proliferation and the higher levels of the transcript for this protein in the hearts of both control and treated fish at 7 dpi relative to 1 dpi suggests that there may be a progressive increase in cardiomyocyte production (Sallin and Jaźwińska, 2016).

Collagen type 1a is a component monomer of collagen in the fish heart and the protein vimentin is used as a marker for fibroblasts, the cells responsible for regulating collagen deposition in most tissues (Chablais et al., 2011; Keen et al., 2016). An increase in the production of these proteins during tissue regeneration would be expected as an increase in collagen production is required for wound healing (Chablais et al., 2011). This response in the injured fish is supported by the higher levels of *col1a1* at 3 and 7 dpi relative to 1 dpi in both the control and T_3 treated group. Additionally, an obvious collagen scar was observed in the damaged zebrafish heart at 7 and 10 dpi in the current study. Although no differences were seen as a result of T_3 treatment at the level of the gene transcript, a greater deposition of collagen in the control group relative to the T_3 treated group is suggested by the higher stiffness seen in AFM measurements of the ventricle cryosections in the control group as mentioned above. In addition, the higher levels of *vimentin* at day 3 in both treatment and control suggests an increase in fibroblast production, however the lower level of this transcript in the hearts from the T_3 treated fish at all time points suggests that thyroid exposure mutes this response. If this is the case, then this implies that the exogenous T_3 treatment is interfering with the normal tissue repair process. Work by Johnston and Gillis (2017) demonstrates that collagen production by trout cardiac fibroblasts is increased after 48 h treatment with exogenous TGF-ß. The higher level *col1a1* at 3dpi and 7dpi relative to 1dpi suggests that there may be a surge in the production of this protein, and, therefore, collagen production following injury.

Loxl1 is a member of the LOX family of enzymes that is involved in collagen crosslinking and the maturation of ECM proteins. Importantly, these enzymes are induced following myocardial infarction and can lead to cardiac fibrosis and dysfunction (González-Santamaría et al., 2016).

In addition, work by Godwin et al. (2017) suggests that dysregulation of these enzymes in a species that can regenerate their heart leads to early maturation of the ECM and is responsible, at least in part, for the inability to replace fibrotic tissue. In the current study, there was a decrease in the transcript levels of *lox1l,* independent of thyroid treatment. This suggests that there would be a decrease in the production of this protein, and, as a result, a decreased capacity to form highly crosslinked scar tissue. Such a response would help ensure that the ECM that forms following an injury is transient and, as a result, does not hinder regeneration.

4.3. T_3 has no direct effect on collagen production by trout cardiac fibroblasts in vitro

Cultured trout cardiac fibroblasts were exposed to exogenous T_3 to determine if the impairment of heart regeneration reported by Hirose et al. (2019) in zebrafish exposed to T_3 may be due, at least in part, to the direct effect of T_3 on collagen production by fibroblasts. The lack of changes in the transcript levels of *mmp2, mmp9, timp2* and *col1a1* and in the abundance of collagen type 1a measured using western blot in the cardiac fibroblasts exposed to T_3 suggests that these cells do not respond directly to changes in T_3 concentrations. Therefore, it appears as though the impairment of heart regeneration caused by increased T_3 levels in a fish species is not due to a direct impact of T_3 on collagen production by fibroblasts. In turn, this suggests that the blunted increase in tissue stiffness at 3 dpi in T_3 exposed zebrafish, compared to that of control, measured using AFM is likely caused by reduced numbers of macrophages and fibroblasts rather than changes in collagen production by individual fibroblasts. This idea is supported by the finding that exposure to T3 for 14 days prior to injury did not cause a difference in stiffness between control and treatment groups at day 0. However, it is also possible that T_3 has an indirect effect on the activity of cardiac fibroblasts *in vivo*. Future investigation into the effects of T_3 on the abundance and activation of fibroblasts post-injury is warranted.

5. Conclusions and perspectives

The results of this work suggest that the comparatively low level of T_3 in zebrafish plays a role in the regenerative capacity of the heart following injury. A reduction in macrophage recruitment to the site of injury in the T_3 treated fish, as suggested by the significantly lower expression of *mpeg1,* is proposed to lead to a reduction in collagen expression and the measured decrease in tissue stiffness. An initial increase in collagen deposition immediately following injury is thought to be a necessary step in tissue repair and the results of this study suggest that a relatively high T_3 level can blunt this response (Sánchez-Iranzo et al., 2018). Further work to determine the relationship between T_3 levels and macrophage recruitment following injury is needed and the results of such studies could contribute to the development of novel therapeutics to increase the regenerative capacity of the mammalian heart.

Funding

This work was funded by the Natural Sciences and Engineering Research Council (NSERC) of Canada. R.L and J.S. were supported by Canada Graduate Scholarships — Master's from NSERC

CRediT authorship contribution statement

Reece R.B. Long: Writing – original draft, Visualization, Methodology, Investigation, Formal analysis, Data curation, Conceptualization. **Oliver M.N. Bullingham:** Visualization, Methodology, Investigation, Data curation. **Benjamin Baylis:** Writing – review & editing, Methodology, Investigation, Formal analysis. **Jared B. Shaftoe:** Writing – review & editing, Visualization, Data curation. **John R. Dutcher:** Writing – review & editing, Supervision, Resources, Methodology. **Todd E. Gillis:** Writing – review & editing, Supervision, Resources, Project administration, Funding acquisition, Conceptualization.

Declaration of competing interest

The authors declare no conflict of interest.

Appendix A. Supplementary data

Supplementary data to this article can be found online at https://doi.org/10.1016/j.cbpa.2024.111769.

Data availability

Data will be made available on request.

References

Alkass, K., Panula, J., Westman, M., Wu, T.-D., Guerquin-Kern, J.-L., Bergmann, O., 2015. No evidence for cardiomyocyte number expansion in preadolescent mice. Cell 163, 1026–1036. https://doi.org/10.1016/j.cell.2015.10.035.

Babaei, F., Ramalingam, R., Tavendale, A., Liang, Y., Yan, L.S.K., Ajuh, P., Cheng, S.H., Lam, Y.W., 2013. Novel blood collection method allows plasma proteome analysis from single Zebrafish. J. Proteome Res. 12, 1580–1590. https://doi.org/10.1021/pr3009226.

Becker, R.O., Chapin, S., Sherry, R., 1974. Regeneration of the ventricular myocardium in amphibians. Nature 248, 145–147. https://doi.org/10.1038/248145a0.

Bergh, J.J., Lin, H.-Y., Lansing, L., Mohamed, S.N., Davis, F.B., Mousa, S., Davis, P.J., 2005. Integrin αVβ3 contains a cell surface receptor site for thyroid hormone that is linked to activation of mitogen-activated protein kinase and induction of angiogenesis. Endocrinology 146, 2864–2871. https://doi.org/10.1210/en.2005-0102.

Brower, G.L., Gardner, J.D., Forman, M.F., Murray, D.B., Voloshenyuk, T., Levick, S.P., Janicki, J.S., 2006. The relationship between myocardial extracellular matrix remodeling and ventricular function. Eur. J. Cardiothorac. Surg. 30, 604–610. https://doi.org/10.1016/j.ejcts.2006.07.006.

Brown, D.D., 1997. The role of thyroid hormone in zebrafish and axolotl development. PNAS 94, 13011–13016.

Candelotti, E., De Vito, P., Ahmed, G., Luly, P.J., Davis, P.Z., Pedersen, J., Lin, H.-Y., Incerpi, S., 2015. Thyroid hormones crosstalk with growth factors: old facts and new hypotheses. Immun, Endo & Metab Agents 15, 71–85.

Ceccarelli, S.M., Chomienne, O., Gubler, M., Arduini, A., 2011. Carnitine palmitoyltransferase (CPT) modulators: a medicinal chemistry perspective on 35 years of research. J. Med. Chem. 54, 3109–3152. https://doi.org/10.1021/jm100809g.

Chablais, F., Jaźwińska, A., 2012a. Induction of myocardial infarction in adult zebrafish using cryoinjury. JoVE e3666. https://doi.org/10.3791/3666.

Chablais, F., Jaźwińska, A., 2012b. The regenerative capacity of the zebrafish heart is dependent on TGFβ signaling. Development 139, 1921–1930. https://doi.org/10.1242/dev.078543.

Chablais, F., Veit, J., Rainer, G., Jaźwińska, A., 2011. The zebrafish heart regenerates after cryoinjury-induced myocardial infarction. BMC Dev. Biol. 11, 1–13. https://doi.org/10.1186/1471-213X-11-21.

Che, X., Huang, Y., Shen, T., Zhong, K., Wei, Y., Fan, G., Jia, K., Yuan, W., Lu, H., 2022. Effect of monosultap on notochord development in zebrafish (*Danio rerio*) embryos. Toxicology 477, 1-10. https://doi.org/10.1016/j.tox.2022.153276.

Davis, P.J., Leonard, J.L., Lin, H.-Y., Leinung, M., Mousa, S.A., 2018. Chapter four - Molecular basis of nongenomic actions of thyroid hormone. In: Litwack, G. (Ed.), Vitamins and Hormones, Thyroid Hormone. Academic Press, pp. 67–96. https://doi.org/10.1016/bs.vh.2017.06.001.

De Vito, P., Incerpi, S., Pedersen, J.Z., Luly, P., Davis, F.B., Davis, P.J., 2011. Thyroid hormones as modulators of immune activities at the cellular level. Thyroid 21, 879–890. https://doi.org/10.1089/thy.2010.0429.

Ferrero, G., Gomez, E., Lyer, S., Rovira, M., Miserocchi, M., Langenau, D.M., Bertrand, J. Y., Wittamer, V., 2020. The macrophage-expressed gene (mpeg) 1 identifies a subpopulation of B cells in the adult zebrafish. J. Leukoc. Biol. 107, 431–443. https://doi.org/10.1002/JLB.1A1119-223R.

Flink, I., 2002. Cell cycle reentry of ventricular and atrial cardiomyocytes and cells within the epicardium following amputation of the ventricular apex in the axolotl, Amblystoma mexicanum : confocal microscopic immunofluorescent image analysis of bromodeoxyuridine-labeled nuclei. Anat. Embryol. 205, 235–244. https://doi.org/10.1007/s00429-002-0249-6.

Franco, M., Chávez, E., Pérez-Méndez, O., 2011. Pleiotropic effects of thyroid hormones: learning from hypothyroidism. J. Thyroid. Res. 2011, e321030. https://doi.org/10.4061/2011/321030.

Garcia-Puig, A., Mosquera, J.L., Jiménez-Delgado, S., García-Pastor, C., Jorba, I., Navajas, D., Canals, F., Raya, A., 2019. Proteomics analysis of extracellular matrix remodeling during zebrafish heart regeneration. Mol. Cell. Proteomics 18, 1745–1755. https://doi.org/10.1074/mcp.RA118.001193.

Gemberling, M., Karra, R., Dickson, A.L., Poss, K.D., 2015. Nrg1 is an injury-induced cardiomyocyte mitogen for the endogenous heart regeneration program in zebrafish. eLife 4, e05871. https://doi.org/10.7554/eLife.05871.

Godwin, J.W., Debuque, R., Salimova, E., Rosenthal, N.A., 2017. Heart regeneration in the salamander relies on macrophage-mediated control of fibroblast activation and the extracellular landscape. Regen. Med. 2, 1–11. https://doi.org/10.1038/s41536-017-0027-y.

González-Rosa, J.M., Martín, V., Peralta, M., Torres, M., Mercader, N., 2011. Extensive scar formation and regression during heart regeneration after cryoinjury in zebrafish. Development 138, 1663–1674. https://doi.org/10.1242/dev.060897.

González-Rosa, J.M., Burns, C.E., Burns, C.G., 2017. Zebrafish heart regeneration: 15 years of discoveries. Regeneration 4, 105–123. https://doi.org/10.1002/reg2.83.

González-Rosa, J.M., Sharpe, M., Field, D., Soonpaa, M.H., Field, L.J., Burns, C.E., Burns, C.G., 2018. Myocardial polyploidization creates a barrier to heart regeneration in Zebrafish. Dev. Cell 44, 433–446. https://doi.org/10.1016/j.devcel.2018.01.021.

González-Santamaría, J., Villalba, M., Busnadiego, O., López-Olañeta, M.M., Sandoval, P., Snabel, J., López-Cabrera, M., Erler, J.T., Hanemaaijer, R., Lara-Pezzi, E., Rodríguez-Pascual, F., 2016. Matrix cross-linking lysyl oxidases are induced in response to myocardial infarction and promote cardiac dysfunction. Cardiovasc. Res. 109, 67–78. https://doi.org/10.1093/cvr/cvv214.

Grivas, D., González-Rajal, Á., Guerrero Rodríguez, C., Garcia, R., de la Pompa, J.L., 2020. Loss of Caveolin-1 and caveolae leads to increased cardiac cell stiffness and functional decline of the adult zebrafish heart. Sci. Rep. 10, 12816. https://doi.org/10.1038/s41598-020-68802-9.

Hirai, M., Cattaneo, P., Chen, J., Evans, S.M., 2016. Revisiting preadolescent cardiomyocyte proliferation in mice. Circ. Res. 118, 916–919. https://doi.org/10.1161/CIRCRESAHA.115.308101.

Hirose, K., Payumo, A.Y., Cutie, S., Hoang, A., Zhang, H., Guyot, R., Lunn, D., Bigley, R. B., Yu, H., Wang, J., Smith, M., Gillett, E., Muroy, S.E., Schmid, T., Wilson, E., Field, K.A., Reeder, D.M., Maden, M., Yartsev, M.M., Wolfgang, M.J., Grützner, F., Scanlan, T.S., Szweda, L.I., Buffenstein, R., Hu, G., Flamant, F., Olgin, J.E., Huang, G. N., 2019. Evidence for hormonal control of heart regenerative capacity during endothermy acquisition. Science 364, 184–188. https://doi.org/10.1126/science.aar2038.

Honkoop, H., de Bakker, D.E., Aharonov, A., Kruse, F., Shakked, A., Nguyen, P.D., de Heus, C., Garric, L., Muraro, M.J., Shoffner, A., Tessadori, F., Peterson, J.C., Noort, W., Bertozzi, A., Weidinger, G., Posthuma, G., Grün, D., van der Laarse, W.J., Klumperman, J., Jaspers, R.T., Poss, K.D., van Oudenaarden, A., Tzahor, E., Bakkers, J., 2019. Single-cell analysis uncovers that metabolic reprogramming by ErbB2 signaling is essential for cardiomyocyte proliferation in the regenerating heart. eLife 8, e50163. https://doi.org/10.7554/eLife.50163.

Hortells, L., Johansen, A.K.Z., Yutzey, K.E., 2019. Cardiac fibroblasts and the extracellular matrix in regenerative and nonregenerative hearts. J. Cardiovas. Dev. Dis. 6, 29. https://doi.org/10.3390/jcdd6030029.

Johnston, E.F., Gillis, T.E., 2017. Transforming growth factor beta-1 (TGF-β1) stimulates collagen synthesis in cultured rainbow trout cardiac fibroblasts. J. Exp. Biol. 220, 2645–2653. https://doi.org/10.1242/jeb.160093.

Johnston, E.F., Gillis, T.E., 2018. Transforming growth factor-β1 induces differentiation of rainbow trout (*Oncorhynchus mykiss*) cardiac fibroblasts into myofibroblasts. J. Exp. Biol. 221, 1–8. https://doi.org/10.1242/jeb.189167.

Junqueira, L.C.U., Bignolas, G., Brentani, R.R., 1979. Picrosirius staining plus polarization microscopy, a specific method for collagen detection in tissue sections. Histochem. J. 11, 447–455. https://doi.org/10.1007/BF01002772.

Keen, A.N., Fenna, A.J., McConnell, J.C., Sherratt, M.J., Gardner, P., Shiels, H.A., 2016. The dynamic nature of hypertrophic and fibrotic remodeling of the fish ventricle. Front. Physiol. 6.

Kimura, W., Xiao, F., Canseco, D.C., Muralidhar, S., Thet, S., Zhang, H.M., Abderrahman, Y., Chen, R., Garcia, J.A., Shelton, J.M., Richardson, J.A., Ashour, A. M., Asaithamby, A., Liang, H., Xing, C., Lu, Z., Zhang, C.C., Sadek, H.A., 2015. Hypoxia fate mapping identifies cycling cardiomyocytes in the adult heart. Nature 523, 226–230. https://doi.org/10.1038/nature14582.

Lai, S.-L., Marín-Juez, R., Moura, P.L., Kuenne, C., Lai, J.K.H., Tsedeke, A.T., Guenther, S., Looso, M., Stainier, D.Y., 2017. Reciprocal analyses in zebrafish and medaka reveal that harnessing the immune response promotes cardiac regeneration. eLife 6, e25605. https://doi.org/10.7554/eLife.25605.

Lavine, K.J., Epelman, S., Uchida, K., Weber, K.J., Nichols, C.G., Schilling, J.D., Ornitz, D.M., Randolph, G.J., Mann, D.L., 2014. Distinct macrophage lineages contribute to disparate patterns of cardiac recovery and remodeling in the neonatal and adult heart. PNAS 111, 16029–16034. https://doi.org/10.1073/pnas.1406508111.

Lazar, M.A., 1993. Thyroid hormone receptors: multiple forms, multiple possibilities*. Endocr. Rev. 14, 184–193. https://doi.org/10.1210/edrv-14-2-184.

LeBert, D., Squirrell, J.M., Freisinger, C., Rindy, J., Golenberg, N., Frecentese, G., Gibson, A., Eliceiri, K.W., Huttenlocher, A., 2018. Damage-induced reactive oxygen species regulate vimentin and dynamic collagen-based projections to mediate wound repair. eLife 7, e30703. https://doi.org/10.7554/eLife.30703.

Lin, D.C., Dimitriadis, E.K., Horkay, F., 2006. Robust strategies for automated afm force curve analysis—I. Non-adhesive indentation of soft, inhomogeneous materials. J. Biomech. Eng. 129, 430–440. https://doi.org/10.1115/1.2720924.

Mujumdar, V.S., Smiley, L.M., Tyagi, S.C., 2001. Activation of matrix metalloproteinase dilates and decreases cardiac tensile strength. Int. J. Cardiol. 79, 277–286. https://doi.org/10.1016/S0167-5273(01)00449-1.

Naqvi, N., Li, M., Calvert, J.W., Tejada, T., Lambert, J.P., Wu, J., Kesteven, S.H., Holman, S.R., Matsuda, T., Lovelock, J.D., Howard, W.W., Iismaa, S.E., Chan, A.Y., Crawford, B.H., Wagner, M.B., Martin, D.I.K., Lefer, D.J., Graham, R.M., Husain, A., 2014. A proliferative burst during preadolescence establishes the final cardiomyocyte number. Cell 157, 795–807. https://doi.org/10.1016/j.cell.2014.03.035.

Nelson, S.N., Van Der Kraak, G., 2010. Characterization and regulation of the insulin-like growth factor (IGF) system in the zebrafish (*Danio rerio*) ovary. Gen. Comp. Endocrinol. 168, 111–120. https://doi.org/10.1016/j.ygcen.2010.04.020.

Notari, M., Ventura-Rubio, A., Bedford-Guaus, S.J., Jorba, I., Mulero, L., Navajas, D., Martí, M., Raya, Á., 2018. The local microenvironment limits the regenerative potential of the mouse neonatal heart. Sci. Adv. 4, eaao5553. https://doi.org/10.1126/sciadv.aao5553.

Page, L., Polok, B., Bustamante, M., Schorderet, D.F., 2013. Bigh3 is upregulated in regenerating zebrafish fin. Zebrafish 10, 36–42. https://doi.org/10.1089/zeb.2012.0759.

Peng, H., Shindo, K., Donahue, R.R., Gao, E., Ahern, B.M., Levitan, B.M., Tripathi, H., Powell, D., Noor, A., Elmore, G.A., Satin, J., Seifert, A.W., Abdel-Latif, A., 2021. Adult spiny mice (Acomys) exhibit endogenous cardiac recovery in response to myocardial infarction. Regen. Med. 6, 1–15. https://doi.org/10.1038/s41536-021-00186-4.

Perrotta, C., Buldorini, M., Assi, E., Cazzato, D., De Palma, C., Clementi, E., Cervia, D., 2014. The thyroid hormone triiodothyronine controls macrophage maturation and functions: protective role during inflammation. Am. J. Pathol. 184, 230–247. https://doi.org/10.1016/j.ajpath.2013.10.006.

Persch, G., Born, Ch., Utesch, B., 1994. Nano-hardness investigations of thin films by an atomic force microscope. Microelectron. Eng. 24, 113–121. https://doi.org/10.1016/0167-9317(94)90061-2.

Porrello, E.R., Mahmoud, A.I., Simpson, E., Hill, J.A., Richardson, J.A., Olson, E.N., Sadek, H.A., 2011. Transient regenerative potential of the neonatal mouse heart. Science 331, 1078–1080. https://doi.org/10.1126/science.1200708.

Poss, K.D., Wilson, L.G., Keating, M.T., 2002. Heart regeneration in zebrafish. Science 298, 2188–2190.

Puente, B.N., Kimura, W., Muralidhar, S.A., Moon, J., Amatruda, J.F., Phelps, K.L., Grinsfelder, D., Rothermel, B.A., Chen, R., Garcia, J.A., Santos, C.X., Thet, S., Mori, E., Kinter, M.T., Rindler, P.M., Zacchigna, S., Mukherjee, S., Chen, D.J., Mahmoud, A.I., Giacca, M., Rabinovitch, P.S., Asaithamby, A., Shah, A.M., Szweda, L.I., Sadek, H.A., 2014. The oxygen-rich postnatal environment induces cardiomyocyte cell-cycle arrest through DNA damage response. Cell 157, 565–579. https://doi.org/10.1016/j.cell.2014.03.032.

Ryan, R., Moyse, B.R., Richardson, R.J., 2020. Zebrafish cardiac regeneration—looking beyond cardiomyocytes to a complex microenvironment. Histochem. Cell Biol. 154, 533–548. https://doi.org/10.1007/s00418-020-01913-6.

Sallin, P., Jaźwińska, A., 2016. Acute stress is detrimental to heart regeneration in zebrafish. Open Biol. 6, 1-15. https://doi.org/10.1098/rsob.160012.

Sánchez-Iranzo, H., Galardi-Castilla, M., Sanz-Morejón, A., González-Rosa, J.M., Costa, R., Ernst, A., Sainz de Aja, J., Langa, X., Mercader, N., 2018. Transient fibrosis resolves *via* fibroblast inactivation in the regenerating zebrafish heart. Proc. Natl. Acad. Sci. USA 115, 4188–4193. https://doi.org/10.1073/pnas.1716713115.

Simões, F.C., Cahill, T.J., Kenyon, A., Gavriouchkina, D., Vieira, J.M., Sun, X., Pezzolla, D., Ravaud, C., Masmanian, E., Weinberger, M., Mayes, S., Lemieux, M.E., Barnette, D.N., Gunadasa-Rohling, M., Williams, R.M., Greaves, D.R., Trinh, L.A., Fraser, S.E., Dallas, S.L., Choudhury, R.P., Sauka-Spengler, T., Riley, P.R., 2020. Macrophages directly contribute collagen to scar formation during zebrafish heart regeneration and mouse heart repair. Nat. Commun. 11, 1–17. https://doi.org/10.1038/s41467-019-14263-2.

Soonpaa, M.H., Zebrowski, D.C., Platt, C., Rosenzweig, A., Engel, F.B., Field, L.J., 2015. Cardiomyocyte cell-cycle activity during preadolescence. Cell 163, 781–782. https://doi.org/10.1016/j.cell.2015.10.037.

Tan, L., Bogush, N., Naib, H., Perry, J., Calvert, J.W., Martin, D.I.K., Graham, R.M., Naqvi, N., Husain, A., 2019. Redox activation of JNK2α2 mediates thyroid hormone-stimulated proliferation of neonatal murine cardiomyocytes. Sci. Rep. 9, 1–15. https://doi.org/10.1038/s41598-019-53705-1.

Tran, C.M., Kim, K.-T., 2020. miR-137 and miR-141 regulate tail defects in zebrafish embryos caused by triphenyl phosphate (TPHP). Environ. Pollut. 262, 1-8. https://doi.org/10.1016/j.envpol.2020.114286.

Vagnozzi, R.J., Maillet, M., Sargent, M.A., Khalil, H., Johansen, A.K.Z., Schwanekamp, J. A., York, A.J., Huang, V., Nahrendorf, M., Sadayappan, S., Molkentin, J.D., 2020. An acute immune response underlies the benefit of cardiac stem cell therapy. Nature 577, 405–409. https://doi.org/10.1038/s41586-019-1802-2.

Whittaker, P., Przyklenk, K., 2009. Fibrin architecture in clots: A quantitative polarized light microscopy analysis. Blood Cells Mol. Dis. 42, 51–56. https://doi.org/10.1016/j.bcmd.2008.10.014.

Zang, L., Shimada, Y., Nishimura, Y., Tanaka, T., Nishimura, N., 2015. Repeated blood collection for blood tests in adult zebrafish. J. Vis. Exp. 102, e53272. https://doi.org/10.3791/53272.

Zena, L.A., Ekström, A., Gräns, A., Olsson, C., Axelsson, M., Sundh, H., Sandblom, E., 2021. It takes time to heal a broken heart: ventricular plasticity improves heart performance after myocardial infarction in rainbow trout, *Oncorhynchus mykiss*. J. Exp. Biol. 224, 1–11. https://doi.org/10.1242/jeb.243578.